Adsorption of Gases on a Carbon Molecular Sieve Used for Air Separation: Linear Adsorptives as Probes for Kinetic Selectivity

ARTICLE *in* LANGMUIR · APRIL 1999

Impact Factor: 4.46 · DOI: 10.1021/la981289p

2 AUTHORS, INCLUDING:

Keith Mark Thomas
Newcastle University
198 PUBLICATIONS **10,403** CITATIONS

Adsorption of Gases on a Carbon Molecular Sieve Used for Air Separation: Linear Adsorptives as Probes for Kinetic Selectivity

C. R. Reid and K. M. Thomas*

Northern Carbon Research Laboratories, Department of Chemistry, Bedson Building, University of Newcastle upon Tyne, Newcastle upon Tyne, NE1 7RU, U.K.

Received September 18, 1998. In Final Form: January 7, 1999

The adsorption of oxygen, nitrogen, and a series of gases/vapors with linear structures (carbon monoxide, carbon dioxide, nitrous oxide, acetylene and carbon disulfide) on a carbon molecular sieve typical of the materials used for air separation were studied over a range of temperatures as a function of pressure in order to understand further the mechanism of air separation. The ratios of the rate constants (k_{O_2}/k_{N_2}) were typically 25 for the carbon molecular sieve used thereby demonstrating the molecular sieving characteristics. The adsorption kinetics obey a linear driving force (LDF) mass transfer model for most of the gases and experimental conditions studied. However there were deviations from the LDF model for carbon dioxide and nitrous oxide. In the case of the former, the kinetic models ranged from LDF through a combined barrier resistance/diffusion model to Fickian diffusion depending on the experimental conditions. The adsorption rate constants increase exponentially with increasing surface coverage for the molecules which follow the LDF model. The barrier resistance kinetic constants derived from the combined barrier resistance/diffusion model also have an exponential dependence on surface coverage. The results are discussed in terms of the mechanism of gas separation using carbon molecular sieves.

Introduction

Carbon molecular sieves (CMS) are used widely for the separation of air into its components.[1,2] These materials have pores of molecular dimensions which provide a relatively high adsorption capacity and kinetic selectivity for various gases. It is generally accepted that the diffusing molecule experiences a net repulsive force on entering the selective porosity, and therefore the molecule must pass over an energy barrier during diffusion into the porosity and this leads to differences in the adsorption kinetics for various gases. The kinetic selectivity for various gases may be controlled by varying the extent of carbon deposition which is used to produce the selective porosity,[1,3] although in some cases, while the rates of adsorption of both oxygen and nitrogen are decreased with increasing extent of carbon deposition, the ratios of the rates are not changed greatly.[4] The difference in the adsorption kinetics of oxygen and nitrogen allows the separation of air into these gases using pressure swing adsorption (PSA). It has been proposed that the difference in the adsorption kinetics of these two gases is mainly related to molecular size with the kinetic diameter of N_2 (0.364 nm) being slightly larger than that of O_2 (0.346 nm).[1] However it is surprising that such a small difference in kinetic diameter should make such a large difference in the rate of adsorption of the two gases, with oxygen adsorbing up to 25 times faster than nitrogen.[3−5]

The selective porosity in carbon molecular sieves prepared by carbon deposition is heterogeneously distributed throughout the microporous material.[3] In the case of these CMS materials it is difficult to quantify the nature of the selective porosity, which is of fundamental importance in assessing the gas separation characteristics of the material. Comparisons of adsorptive dimensions have not proved to be a good guide to adsorption kinetics for a wide range of adsorptives. Previous studies have involved the calculation of critical pore dimensions when the pore dimensions give zero interaction potentials for the adsorptive to assess the relative orders of the rates of adsorption for a range of adsorptives.[6,7] This appears to provide a better correlation than comparison of the adsorptive dimensions. However in the real situation the selective porosity in the CMS provides a barrier to the diffusion of a range of adsorptives, and the barriers need to be quantified to the limit where exclusion of the molecules from the porous structure is observed. Previous work has focused on the adsorption characteristics of oxygen, nitrogen, and also the noble gases, neon, argon, and krypton on a CMS prepared by carbon deposition on a microporous substrate.[5,8] The spherical adsorptives were used to investigate the effect of the size of a molecule on the rate of adsorption on the CMS. In the case of linear adsorptives such as nitrogen and oxygen, at least some loss of rotational freedom occurs since it is likely that the molecule passes through the selective porosity along its minimum dimension, and this factor needs to be quantified.

In this study the adsorption of linear molecules has been investigated to determine the relative importance of factors such as molecular size, shape, and electronic structure in determining the adsorption kinetics of gases on carbon molecular sieves. The gases studied include carbon monoxide, acetylene, nitrous oxide, and carbon

* To whom correspondence should be addressed. E-mail: mark.thomas@ncl.ac.uk.

(1) Armor, J. N. In *Separation Technology*; Vansat, E. F., Ed.; Elsevier Science B.V., Amsterdam, 1994; p 163.
(2) Verma, S. K. *Carbon* **1991**, *29*, 793.
(3) Chagger, H. K.; Ndaji, F. E.; Sykes, M. L.; Thomas, K. M. *Carbon* **1995**, *33*, 1405.
(4) Chihara, K.; Suzuki, M. *Carbon* **1979**, *17*, 339.
(5) Reid, C. R.; O'Koye, I. P.; Thomas, K. M. *Langmuir* **1998**, *14*, 2415.
(6) Rao, M. B.; Jenkins, R. G.; Steele, W. A. *Ext. Abstr. Program—Biennial Conf. Carbon, 17th*, **1985**, 114.
(7) Rao, M. B.; Jenkins, R. G.; Steele, W. A. *Langmuir* **1985**, *1*, 137.
(8) O'koye, I. P.; Benham, M.; Thomas, K. M. *Langmuir* **1997**, *13*, 4054.

10.1021/la981289p CCC: $18.00
Published on Web 03/27/1999

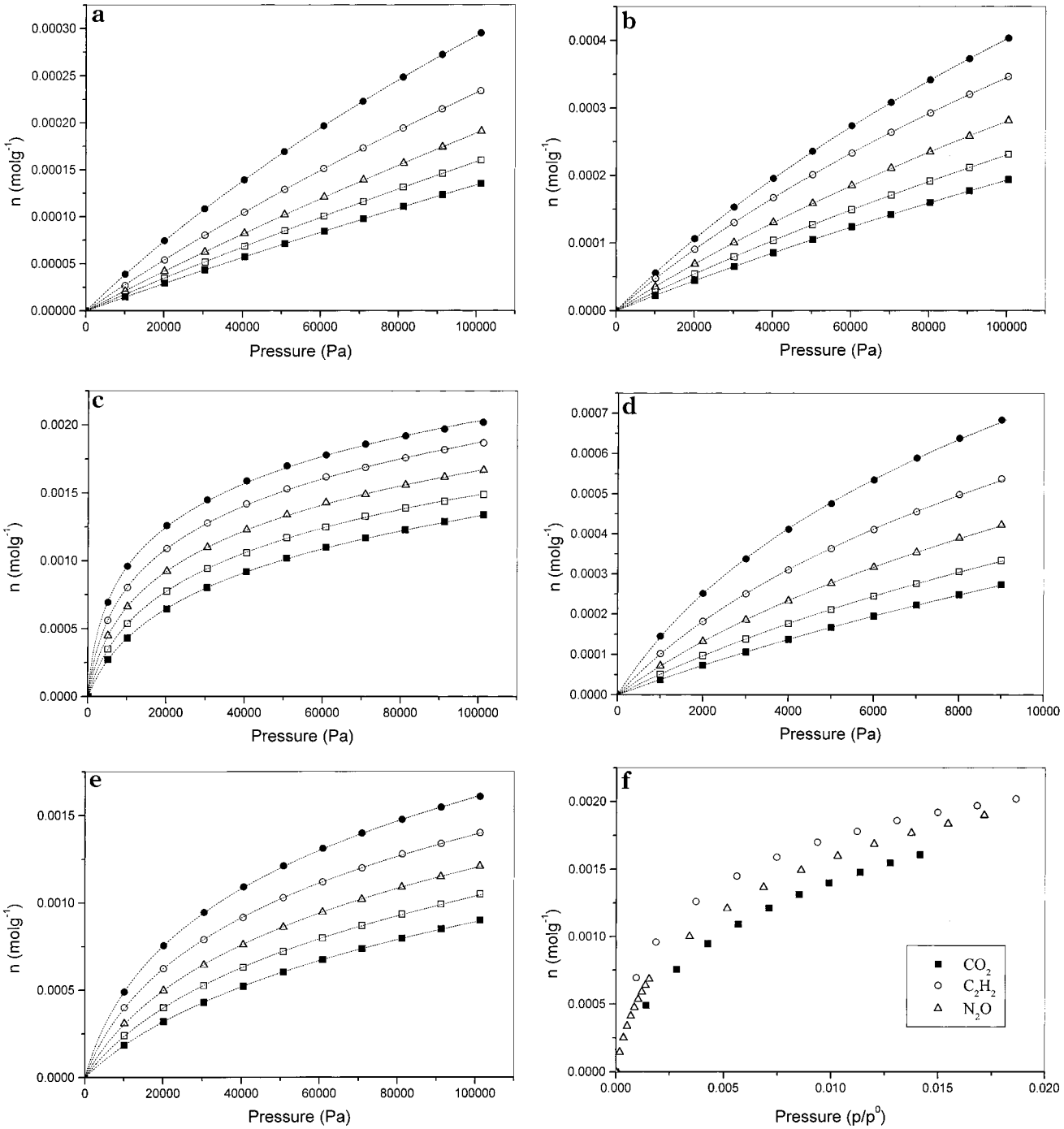

Figure 1. (a) Adsorption isotherms for nitrogen on carbon molecular sieve CMS A: temperature range 303−343 K, 0−100 kPa (303 K, ●; 313 K, ○; 323 K, △; 333 K, □; 343 K, ■; - - -, calculated from virial parameters). (b) Adsorption isotherms for carbon monoxide on carbon molecular sieve CMS A: temperature range 303−343 K, 0−100 kPa (303 K, ●; 313 K, ○; 323 K, △; 333 K, □; 343 K, ■; - - -, calculated from virial parameters). (c) Adsorption isotherms for acetylene on carbon molecular sieve CMS A: temperature range 303−343 K, 0−100 kPa (303 K, ●; 313 K, ○; 323 K, △; 333 K, □; 343 K, ■; - - -, calculated from virial parameters). (d) Adsorption isotherms for nitrous oxide on carbon molecular sieve CMS A: temperature range 303−343 K, 0−9 kPa (303 K, ●; 313 K, ○; 323 K, △; 333 K, □; 343 K, ■; - - -, calculated from virial parameters). (e) Adsorption isotherms for carbon dioxide on carbon molecular sieve CMS A: temperature range 303−343 K, 0−100 kPa (303 K, ●; 313 K, ○; 323 K, △; 333 K, □; 343 K, ■; - - -, calculated from virial parameters). (f) Adsorption isotherms for carbon dioxide, nitrous oxide, and acetylene at 303 K on a p/p^0 basis.

dioxide. The adsorption of carbon disulfide vapor on the CMS was also investigated for comparison with carbon dioxide. The adsorption kinetics for each gas/vapor were studied as a function of temperature and pressure, and the activation energies and preexponential factors were determined. The isosteric heats of adsorption were also obtained for the gases studied. The results are compared with those of oxygen and nitrogen and discussed in terms of the mechanism of adsorption in microporous materials.

Experimental Section

Materials Used. The commercial carbon molecular sieve (CMS A) used in this study was supplied by Air Products and Chemicals Inc., U.S. The CMS was prepared by carbon deposition on a microporous substrate. The gases used were supplied by BOC Ltd. and had the following purities: nitrogen (99.999%), carbon monoxide (99.95%), nitrous oxide (99.997%), acetylene (99.95%), and carbon dioxide (99.999%). The carbon disulfide was obtained from Aldrich Chemicals Inc. It was 99.9% pure and

Table 1. Virial Constants for Adsorption of Nitrogen, Carbon Monoxide, Carbon Dioxide, Nitrous Oxide, and Acetylene on the Carbon Molecular Sieve: Temperature Range 303−343 K

	A_0/ln(mol g^{-1} Pa^{-1})				
temp/K	nitrogen (0−100 kPa)	carbon monoxide (0−100 kPa)	acetylene (0−100 kPa)	nitrous oxide (0−9 kPa)	carbon dioxide (0−100 kPa)
303	−19.336 ± 0.002	−18.963 ± 0.002	−14.781 ± 0.027	−15.588 ± 0.010	−16.344 ± 0.005
313	−19.684 ± 0.001	−19.126 ± 0.001	−15.240 ± 0.012	−15.986 ± 0.007	−16.637 ± 0.008
323	−19.957 ± 0.002	−19.425 ± 0.001	−15.635 ± 0.007	−16.371 ± 0.005	−16.995 ± 0.007
333	−20.150 ± 0.001	−19.684 ± 0.001	−16.037 ± 0.005	−16.730 ± 0.003	−17.326 ± 0.008
343	−20.334 ± 0.001	−19.895 ± 0.001	−16.405 ± 0.005	−17.054 ± 0.002	−17.635 ± 0.006
	A_1/(g mol^{-1})				
temp/K	nitrogen (0−100 kPa)	carbon monoxide (0−100 kPa)	acetylene (0−100 kPa)	nitrous oxide (0−9 kPa)	carbon dioxide (0−100 kPa)
303	−1077 ± 7	−914 ± 6	−1444 ± 17	−943 ± 13	−1000 ± 4
313	−851 ± 7	−1037 ± 5	−1366 ± 8	−1151 ± 15	−1045 ± 8
323	−684 ± 16	−954 ± 7	−1364 ± 6	−1204 ± 16	−1035 ± 8
333	−707 ± 12	−887 ± 2	−1330 ± 5	−1223 ± 20	−1024 ± 11
343	−726 ± 6	−883 ± 3	−1302 ± 5	−1194 ± 21	−1012 ± 9

benzene free and was further purified by distillation and drying over phosphorus pentoxide.

Measurement of Adsorption Kinetics. The kinetic measurements were carried out using the intelligent gravimetric analyzer (IGA) supplied by Hiden Analytical, Ltd. The instrument has been described in detail previously.[9] The balance and pressure control system are fully thermostated to 0.2 K to eliminate the effects of changes in the external environment. The IGA instrument is a fully computerized microbalance which allows the adsorption−desorption isotherms and the corresponding kinetics of adsorption or desorption at each pressure step to be determined with the approach to equilibrium being monitored in real time using a computer algorithm.[5,8,9] This allowed the measurement of adsorption kinetics for different amounts of preadsorbed gas/vapor. The microbalance had a long-term stability of ±1 μg with a weighing resolution of 0.2 μg. The pressure was monitored by two pressure transducers with ranges of 0−10 kPa and 0−1 MPa. The pressure increments typically took 30 s, and therefore the period over which the pressure change occurred was very small compared with the adsorption kinetics. The accuracy of the set-point regulation was ±0.02% of the range used. The pressure was maintained at the set point by active computer control of inlet/outlet valves throughout the duration of the kinetic experiments. The sample temperature was measured at ∼5 mm from the sample and was controlled to ±0.05 K throughout the duration of the experiment. The carbon sample (∼0.5 g) was outgassed to a constant weight at 443 K and 10^{-5} Pa prior to measurement of the isotherms. The initial pressure increment from high vacuum ($<10^{-5}$ Pa) resulted in a change of temperature of 0.5 K due to the introduction of conduction from the thermostatically controlled water jacket through the gas to the sample.

Results

Adsorption Capacities. Adsorption isotherms of nitrogen, carbon monoxide, acetylene, nitrous oxide, and carbon dioxide over the temperature range 303−343 K are shown in parts a−e of Figure 1, respectively. Nitrous oxide was studied in detail over the pressure range 0−9 kPa, whereas the other gases were studied over the pressure range 0−100 kPa. The uptakes of all gases as a function of pressure were approximately linear at low pressures, but deviations from linearity were observed as pressure increases. The adsorption temperatures used in this study were well above the critical temperatures for carbon monoxide and nitrogen, while at 303 K acetylene, nitrous oxide, and carbon dioxide were just below their critical temperatures. Therefore the isotherms of these three gases at 303 K were compared with each other on a relative pressure (p/p^o) basis (see Figure 1f) to assess

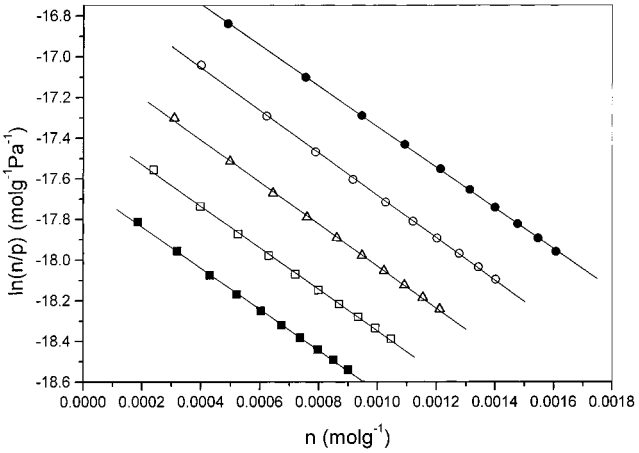

Figure 2. Virial graphs for the adsorption of carbon dioxide on carbon molecular sieve CMS A: temperature range 303−343 K, 0−100 kPa (303 K, ●; 313 K, ○; 323 K, △; 333 K, □; 343 K, ■).

micropore volumes and surface areas. It is apparent that the isotherms are similar. The isotherms were typically repeatable to better than ±1%. Desorption studies showed that the isotherms were reversible.

It was necessary to use a virial equation approach to compare the isotherms measured at higher temperatures. The virial equation can be written in the form

$$\ln(n/p) = A_0 + A_1 n + A_2 n^2 + \ldots \quad (1)$$

where n is the amount adsorbed at pressure p and the first virial coefficient A_0 is related to the Henry's law constant K_0 by the equation $K_0 = \exp(A_0)$.[10] K_0 is dependent on the interaction between the adsorbent surfaces and the adsorbed gas molecules. The statistical mechanics interpretation of the virial parameter A_1 relates it to interaction between pairs of molecules under the influence of surface forces. The relation between A_1 and the two-dimensional second virial coefficient B_{2D} for adsorption on a homogeneous surface is $A_1 = -2B_{2D}/A_s$, where A_s is the surface area of the adsorbent. In the case of microporous adsorbents the interpretation of B_{2D} is more complex. In this study analysis of the data showed that the higher terms (A_2, etc.) in the virial equation could be ignored. The virial graphs for carbon dioxide are clearly

(9) Benham, M.; Ross, D. K. *Z. Phys.* **1989**, *25*, 163.

(10) Cole, J. H.; Everett, D. H.; Marshall, C. T.; Paniego, A. R.; Powl, J. C.; Rodriguez-Reinoso, F. *J. Chem. Soc., Faraday Trans. 1* **1974**, *70*, 2154.

Table 2. Comparison of Isosteric Heats of Adsorption Q_{st} (kJ mol^{-1}) Obtained from the Determination of the Henry's Law Constant (K_0) from the Virial Equation with Literature Values

gas	this work	graphite basal plane (ref 7)	microporous carbons and CMS
nitrogen	21.5 ± 1.5	9.2	18.8 (ref 30) 14.7−15.9 (ref 29) 16.2−17.9 (ref 10) 11.7−15.9 (ref 2)
oxygen	22.0 ± 1.6 (ref 5)	10.5	17.2 (ref 30) 11.7−15.9 (ref 2)
carbon monoxide	19.9 ± 0.6	10.8	
carbon dioxide	28.4 ± 0.7	16.7	
nitrous oxide	31.8 ± 0.1		
acetylene	35.0 ± 0.2		
argon	17.7 ± 0.2 (ref 5)	9.6	14.9−17.3 (ref 10) 16.8 (ref 30)

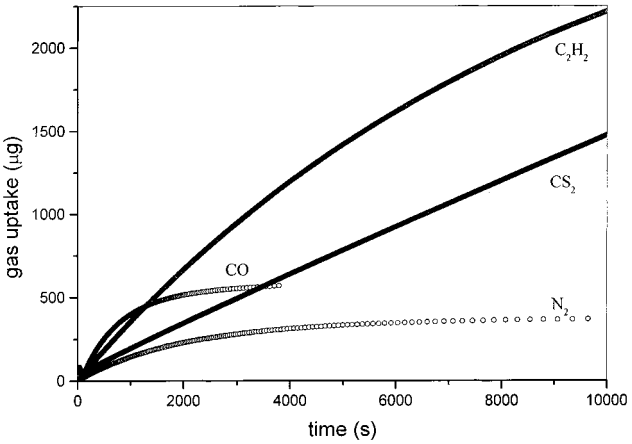

Figure 3. Variation of the gas uptake with time for the adsorption of (a) carbon monoxide (313 K, 20−30 kPa), (b) nitrogen (313 K, 20−30 kPa), (c) acetylene (313 K, 20−30 kPa), and (d) carbon disulfide (343 K, 0−0.1 kPa) on CMS A.

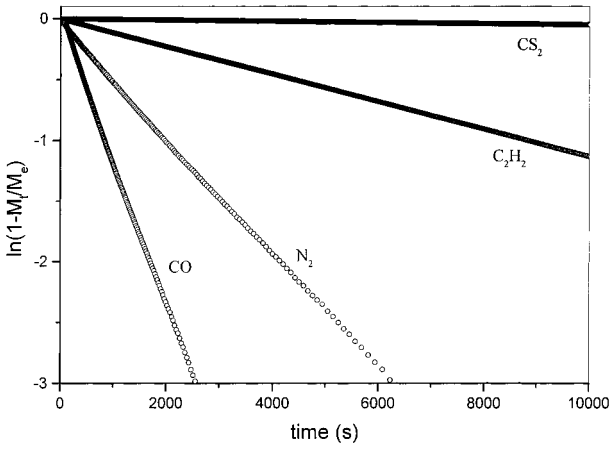

Figure 4. Variation of $\ln(1 - M_t/M_e)$ against time for the adsorption of carbon monoxide (313 K, 20−30 kPa), nitrogen (313 K, 30−40 kPa), acetylene (313 K, 20−30 kPa), and carbon disulfide (343 K, 0−0.1 kPa) on CMS A.

linear and have similar second virial coefficients (A_1) as shown in Figure 2. The virial graphs for nitrogen, carbon monoxide, nitrous oxide, and acetylene were similar. The virial parameters obtained from these graphs are shown in Table 1. The parameters for nitrogen are in very good agreement with those obtained previously for the pressure range 0−9 kPa.[5] The values of the first virial coefficient (A_0) for carbon dioxide, nitrous oxide, and acetylene were

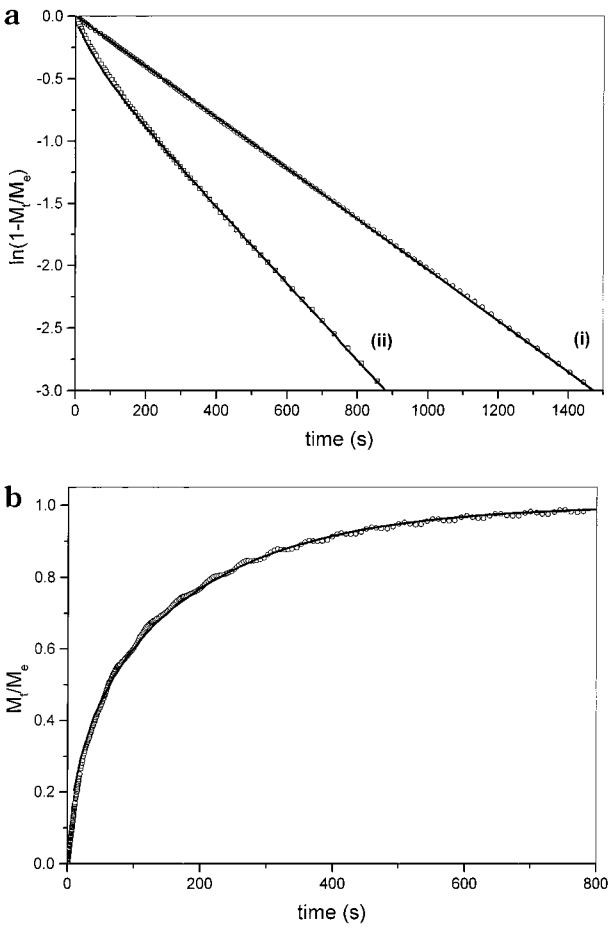

Figure 5. (a) Comparison of the $\ln(1 - M_t/M_e)$ versus time graph for carbon dioxide uptake on CMS A with kinetic models: (i) experimental data (every 20th data point) and calculated from the linear driving force model for pressure increment 0−10 kPa, 313 K (—); (ii) experimental data (every 10th data point) and the combined barrier resistance/diffusion model for pressure increment 40−50 kPa, 313 K. (—). (b) Comparison of the M_t/M_e versus time graph for carbon dioxide uptake on CMS A for pressure increment 90−100 kPa, 343 K, with the calculated profile (—) for Fickian diffusion into a spherical particle.

much higher than those for nitrogen, oxygen, argon,[5,8] and carbon monoxide as a result of the higher extents of adsorption. The values of the second virial parameter A_1 for the gases studied were in the range 600−1450 g mol^{-1} over the temperature range 303−343 K. The A_1 parameter for nitrogen adsorption decreased significantly with increasing temperature. In contrast, the values for the virial parameter A_1 for carbon monoxide, carbon dioxide, and nitrous oxide were similar over the temperature range studied with only weak trends with temperature. The A_1 virial parameters for acetylene were higher than those for the other gases studied but did not vary greatly with temperature.[5,8] Acetylene is a highly quadrupolar molecule, and this results in the high value of A_1. The isotherms calculated from the virial coefficients for each gas are compared with the experimental isotherms in Figure 1a−e, and it can be seen that there is excellent agreement.

The values for the isosteric heats of adsorption (Q_{st}) for the gases studied obtained from graphs of $\ln(A_o)$ versus $1/T$ are given in Table 2. The limiting values of Q_{st} at zero surface coverage for N_2 and CO were 21.5 ± 1.5 and 19.9 ± 0.6 kJ mol^{-1}, while values for the larger linear molecules carbon dioxide, nitrous oxide, and acetylene were 28.4 ± 0.7, 31.8 ± 0.1, and 35.0 ± 0.2 kJ mol^{-1}, respectively. The

Table 3. Kinetic Data ($k/(10^{-4}$ s$^{-1})$) for Nitrogen Adsorption on CMSA: Temperature Range 303−343 K; Pressure Range 0−100 kPa

temp/K	0−10 kPa	10−20 kPa	20−30 kPa	30−40 kPa	40−50 kPa	50−60 kPa	60−70 kPa	70−80 kPa	80−90 kPa	90−100 kPa
303	2.85 ± 0.02	2.83 ± 0.01	3.02 ± 0.01	3.12 ± 0.01	3.29 ± 0.01	3.43 ± 0.01	3.51 ± 0.01	3.67 ± 0.01	3.86 ± 0.02	3.98 ± 0.01
313	4.70 ± 0.01	4.59 ± 0.02	4.91 ± 0.02	5.06 ± 0.02	5.24 ± 0.02	5.38 ± 0.02	5.57 ± 0.02	5.75 ± 0.03	5.95 ± 0.03	6.08 ± 0.03
323	7.81 ± 0.02	7.91 ± 0.02	8.19 ± 0.02	8.28 ± 0.03	8.52 ± 0.04	8.64 ± 0.04	8.78 ± 0.05	9.14 ± 0.04	9.41 ± 0.05	9.60 ± 0.04
333	12.62 ± 0.04	12.82 ± 0.04	12.95 ± 0.08	12.96 ± 0.09	13.44 ± 0.07	13.73 ± 0.08	14.14 ± 0.08	14.38 ± 0.09	14.62 ± 0.09	14.82 ± 0.10
343	20.15 ± 0.09	20.33 ± 0.15	20.49 ± 0.11	20.87 ± 0.11	20.93 ± 0.13	21.22 ± 0.14	21.92 ± 0.14	21.83 ± 0.12	22.62 ± 0.12	23.45 ± 0.14

values of Q_{st} obtained for adsorption of nitrogen and carbon monoxide on the CMS were similar to those for oxygen, argon, and krypton.

Adsorption Kinetics. Graphs of adsorption versus time for nitrogen, carbon monoxide, acetylene, and carbon disulfide are shown in Figure 3. This illustrates the similar shapes of the adsorption uptake versus time for a range of pressure increments and also the differences in the rates of adsorption. A variety of models based on Fickian,[11] linear driving force (LDF),[5,12] a combined barrier resistance/Fickian diffusion model,[13] and Langmuir type second-order kinetics[14−16] have been used to describe the adsorption kinetics in porous materials and carbon molecular sieves. In this study the first three models provide satisfactory descriptions of the adsorption kinetics of the various gases depending on the experimental conditions.

The LDF model is described by the following equation

$$M_t/M_e = 1 - \exp(-kt) \qquad (2)$$

where M_t = mass uptake at time t, M_e = mass uptake at equilibrium, and k is the kinetic rate constant. Graphs of $\ln(1 - M_t/M_e)$ against time for the uptake of the gases are shown in Figure 4. These graphs are linear for nitrogen, carbon monoxide, acetylene, and carbon disulfide adsorption, clearly showing that these gases follow a linear driving force (LDF) mass transfer kinetic model,[3,5,12] and the kinetic data are given in Tables 3, 4, and 5, respectively. The adsorption kinetics can be compared in terms of the rate constant (k) for the LDF model, which is determined from the gradient of the kinetic plot as shown in Figure 4 or by fitting the adsorption uptake curves to eq 2. In the case of carbon dioxide the gas uptake graphs for the 0−10 kPa steps at 303 and 313 K follow the LDF model, while the adsorption kinetics for 10 kPa steps at higher pressures deviate as shown in Figure 5a. Therefore the LDF model may only be used as an approximate description of the carbon dioxide adsorption kinetics at higher pressures.

A combined barrier resistance/diffusion model is based on the existence of a barrier resistance at the surface and subsequent diffusion in a spherical microporous system by Fick's law.[13] The relevant equations for isothermal diffusion into a spherical particle with this model are

$$\frac{\partial C}{\partial t} = D\left(\frac{\partial^2 C}{\partial r^2}\right) + \left(\frac{2}{r}\right)\left(\frac{\partial C}{\partial r}\right) \qquad (3)$$

where D is the crystallite diffusivity (cm^2 s^{-1}), C is the sorbate concentration in the crystallite (mmol cm^{-3}), r is the radial coordinate, and t is the time.

$$D = \frac{\partial C(r_c t)}{\partial r} = k_b\{C^*(t) - C(r,t)\} \qquad (4)$$

where D is the crystallite diffusivity (cm^2 s^{-1}), k_b is the barrier resistance (cm s^{-1}), r_c is the radius of the particle (cm), r is the radial coordinate, t is time, C is the sorbate concentration in crystallite (mmol cm^{-3}), and C^* is the surface concentration in equilibrium with gas phase (mmol cm^{-3}). The parameters derived from the model are k_b the barrier resistance constant and k_d, which is equal to D/r_c^2. A fully implicit (backward-time) difference scheme was used to represent the diffusion equation in the appropriate coordinate system. A uniform grid of 100 points was employed for a sphere. The matrix equations at each time step were solved by the standard tridiagonal algorithm.[17] To model finite slabs, a 41 × 41 × 41 spatial grid was used and the matrix equations at each time step were solved by successive over relaxation. A combined barrier resistance/diffusion model provides a suitable model for the adsorption kinetic data for the 40−50 kPa pressure increment as shown by a comparison of the experimental data and the calculated values obtained for the model (see graph ii, Figure 5a).

Fick's law for isothermal diffusion into a homogeneous sphere is given by eq 3. The solution to this equation is:

$$\frac{M_t}{M_e} = 1 - \frac{6}{\pi^2}\sum_{n=1}^{\infty}\left(\frac{1}{n^2}\right)\exp\left(\frac{-Dn^2\pi^2 t}{r^2}\right) \qquad (5)$$

where M_t = mass uptake at time t, M_e = mass uptake at equilibrium, D = diffusivity, and r = radius of the particle. The above series converges very rapidly, and a graph of $\ln(1 - M_t/M_e)$ versus time is close to linearity in the uptake region $M_t/M_e > 0.6$. Therefore the graph only differs from the LDF model in the initial uptake region where $M_t/M_e < 0.6$. A comparison of the adsorption of carbon dioxide on CMS A at 343 K for pressure increment 90−100 kPa with the Fickian diffusion model for a spherical particle is shown in Figure 5b. It is evident that the adsorption kinetics follow a Fickian model under these conditions. Therefore the adsorption of carbon dioxide on CMS A follows kinetic models which range from linear driving force through a combined barrier resistance/diffusion model to a Fickian model depending on the experimental conditions.

The adsorption kinetics for nitrous oxide adsorption on CMS A deviate to a greater extent from the LDF model than carbon dioxide but can also be described in terms of a combined barrier resistance/diffusion model for the lower temperature region (303−323 K). A typical graph of $\ln(1 - M_t/M_e)$ versus time, where M_t and M_e are the mass uptakes at time t and equilibrium for nitrous oxide adsorption is shown in Figure 6a, together with the calculated profile from the combined barrier resistance/

(11) Crank, J. *The Mathematics of Diffusion*, 2nd ed.; Clarendon Press: Oxford, 1975.
(12) Braymer, T. A.; Coe, C. G.; Farris, T. S.; Gaffney, T. R.; Schork, J. M.; Armor, J. N. *Carbon* **1994**, *32*, 445.
(13) Loughlin, K. F.; Hassan, M. M.; Fatehi, A. I.; Zahur, M. *Gas Sep., & Pur.*, **1993**, *7*, 264.
(14) LaCava, A. I.; Dominguez, J.; Cardenas, J. *Ads. Sci.and Technol.* **1988**, *158*, 323.
(15) LaCava, A. I.; Koss, V. A.; Wickens, D. *Gas Sep. Purif.* **1989**, *3*, 180.
(16) Dominguez, J.A.; Psaras, D.; LaCava, A. I. *AIChE Symp. Ser.* **1988**, *84*, 73.
(17) Press, W. H.; Teukolsky, S. A.; Vetterling, W. T.; Flannery, B. P. *Numerical recipes in Fortran*; Cambridge University Press: Cambridge, 1992; Chapter 19.

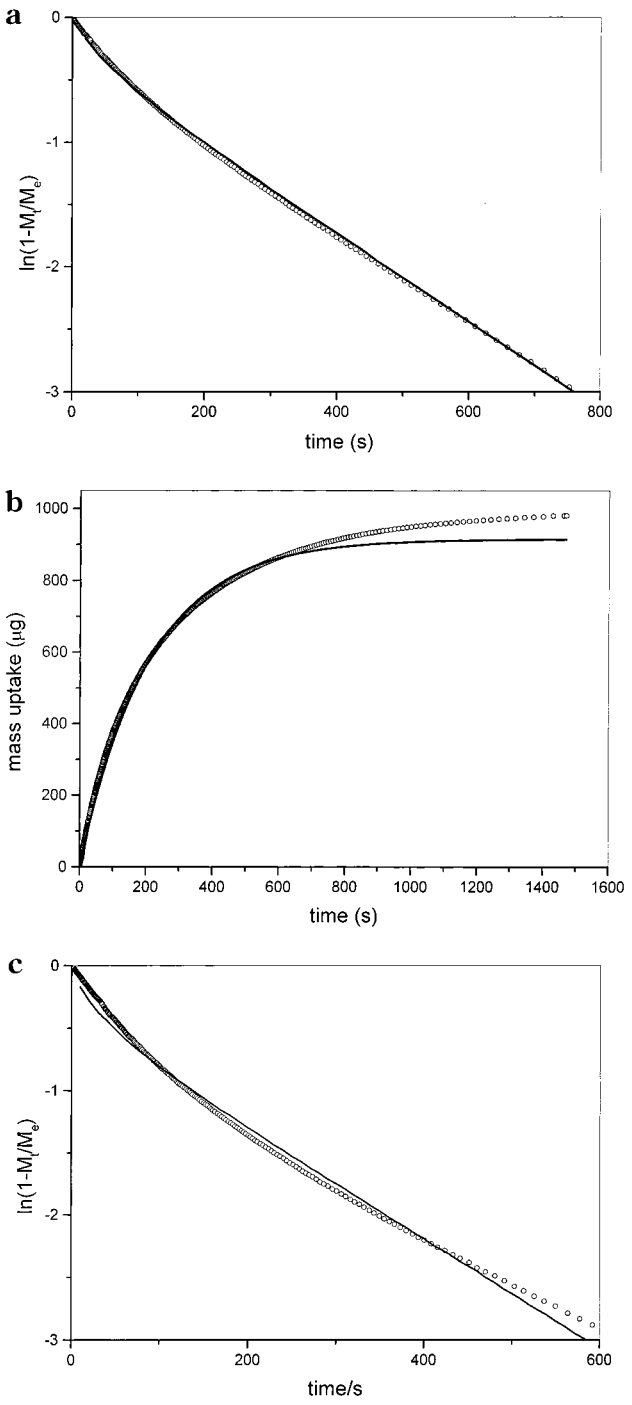

Figure 6. (a) Variation of $\ln(1 - M_t/M_e)$ against time for the adsorption of nitrous oxide at 313 K for pressure increment 7−8 kPa (every second data point) with the calculated profile (—)for the combined barrier resistance/Fickian diffusion model. (b) A comparison of the uptake of nitrous oxide on CMS A (7−8 kPa, 313 K) with the calculated profile (—) from the LDF model. (c) Variation of $\ln(1 - M_t/M_e)$ against time for the adsorption of nitrous oxide at 333 K for pressure increment 8−9 kPa with the calculated profile (—) for the combined barrier resistance/ Fickian diffusion model.

diffusion model. It is apparent that the combined barrier resistance/diffusion model provides a good description for nitrous oxide adsorption on CMS A in this case. A comparison of the experimental data in Figure 6a with the LDF model is shown in Figure 6b. It is apparent that the largest deviations occur in the final stages ($M_t/M_e >$ 0.85) of gas uptake. The graph of $\ln(1 - M_t/M_e)$ versus time for nitrous oxide adsorption for the pressure incre-

Table 4. Kinetic Data ($k/(10^{-4}$ s^{-1})) for Carbon Monoxide Adsorption on CMSA: Temperature Range 303−343 K; Pressure Range 0−100 kPa

temp/K	0−10 kPa	10−20 kPa	20−30 kPa	30−40 kPa	40−50 kPa	50−60 kPa	60−70 kPa	70−80 kPa	80−90 kPa	90−100 kPa
303	6.969 ± 0.011	7.478 ± 0.017	7.993 ± 0.018	8.544 ± 0.021	8.875 ± 0.023	9.378 ± 0.024	9.978 ± 0.033	10.407 ± 0.032	10.793 ± 0.045	10.964 ± 0.047
313	11.94 ± 0.03	12.46 ± 0.04	13.31 ± 0.04	13.82 ± 0.05	14.75 ± 0.05	15.37 ± 0.06	15.76 ± 0.07	16.69 ± 0.08	17.36 ± 0.07	17.94 ± 0.09
323	19.07 ± 0.06	19.38 ± 0.07	20.24 ± 0.08	21.46 ± 0.09	22.15 ± 0.08	22.96 ± 0.12	23.84 ± 0.12	25.15 ± 0.12	26.08 ± 0.09	25.88 ± 0.11
333	30.24 ± 0.15	30.59 ± 0.14	31.34 ± 0.16	32.96 ± 0.16	34.54 ± 0.15	34.42 ± 0.20	35.16 ± 0.18	38.07 ± 0.19	37.91 ± 0.17	37.84 ± 0.02
343	47.55 ± 0.29	46.66 ± 0.26	48.38 ± 0.33	49.75 ± 0.37	51.60 ± 0.37	51.68 ± 0.40	53.51 ± 0.40	55.10 ± 0.33	55.31 ± 0.30	55.19 ± 0.33

ment 7−8 kPa at 333 K is shown in Figure 6c. It is evident the combined barrier resistance/diffusion model for the adsorption kinetics for nitrous oxide on CMS A was less satisfactory. The kinetic data obtained from the combined barrier resistance/diffusion model for the adsorption of nitrous oxide at 333 and 343 K have not been included because of the deviation from the model leads to larger uncertainties in the kinetic parameters. If the experimental data in Figure 6c are compared with the LDF model, it is evident that the model deviates to the greatest extent in the final stages of uptake.

The full kinetic data for the adsorption of the various probe molecules are presented in Tables 3−8. When comparisons of rates of adsorption are made at the same surface coverage, it can be seen that carbon monoxide is 2−3 times faster than that of nitrogen adsorption despite having a very similar activation energy. Nitrous oxide adsorption is ∼1.5−2 times faster than carbon dioxide adsorption and ∼10 times faster than nitrogen adsorption. The adsorption kinetics for acetylene were much slower than that for nitrogen while carbon disulfide adsorption was very slow. In the case of carbon disulfide adsorption on CMS A, equilibrium was achieved over a period of approximately 1 week at the highest temperatures studied. Therefore the long equilibrium times prevented the collection of isotherm data for carbon disulfide adsorption.

Discussion

The structures and intermolecular interactions of monolayers of linear molecules adsorbed on the graphite basal plane have been reviewed in detail.[18] While these observations refer to low temperatures, they show the significance of intermolecular interactions in determining the structure of the adsorbed phase. The suite of linear molecules used in the study of the adsorption characteristics of carbon molecular sieve used for air separation have a range of properties. Selected structural, physical, and electronic energy parameters[1,18−23] are shown in Table 9. Nitrogen has important electrostatic quadrupolar interactions whereas the interactions in oxygen are negligible. Carbon monoxide is very similar to nitrogen in terms of its bond length and interaction potentials. Both carbon monoxide and nitrous oxide have dipoles, but these are negligibly small. Carbon dioxide is also strongly quadrupolar.[18] The nitrous oxide molecule is very similar in size and strength of intermolecular interactions to carbon dioxide. Carbon disulfide is much larger than carbon dioxide while acetylene is a very strongly quadrupolar molecule. These differences in size and electronic structure need to be considered in relation to the adsorption kinetics of the adsorptives on the CMS.

Adsorption Isotherms. The adsorptions of carbon dioxide, nitrous oxide, and acetylene at 303 K are below the critical temperatures of the gases, and therefore the adsorption isotherms in these cases may be described on a p/p^0 basis and compared with the data from carbon dioxide adsorption at 273 K, which is frequently used as a method for estimation of the micropore volumes and surface areas in microporous materials.[24] This comparison

Table 5. Kinetic Data ($k/(10^{-4}$ s^{-1})) for Acetylene Adsorption on CMSA: Temperature Range 303−343 K; Pressure Range 0−100 kPa

temp/K	0−5 kPa	5−10 kPa	10−20 kPa	20−30 kPa	30−40 kPa	40−50 kPa	50−60 kPa	60−70 kPa	70−80 kPa	80−90 kPa	90−100 kPa
303	0.147 ± 0.001	0.308 ± 0.001	0.527 ± 0.001	0.827 ± 0.001	1.099 ± 0.001	1.406 ± 0.001	1.708 ± 0.002	2.003 ± 0.002	2.313 ± 0.004	2.713 ± 0.005	3.009 ± 0.025
313	0.232 ± 0.001	0.438 ± 0.001	0.740 ± 0.001	1.115 ± 0.001	1.453 ± 0.001	1.863 ± 0.003	2.210 ± 0.003	2.436 ± 0.005	2.964 ± 0.006	3.388 ± 0.004	3.721 ± 0.007
323	0.367 ± 0.001	0.628 ± 0.001	0.984 ± 0.001	1.457 ± 0.002	1.862 ± 0.001	2.272 ± 0.001	2.600 ± 0.005	3.716 ± 0.015	3.483 ± 0.006	4.039 ± 0.006	4.505 ± 0.010
333	0.587 ± 0.001	0.952 ± 0.001	1.435 ± 0.001	2.044 ± 0.007	2.597 ± 0.001	3.068 ± 0.005	3.745 ± 0.004	4.230 ± 0.006	5.052 ± 0.007	5.403 ± 0.009	6.033 ± 0.011
343	0.909 ± 0.001	1.371 ± 0.001	2.005 ± 0.001	2.710 ± 0.002	3.425 ± 0.003	4.061 ± 0.004	4.838 ± 0.006	5.450 ± 0.007	6.132 ± 0.009	6.844 ± 0.008	7.551 ± 0.013

(18) Steele, W. A. *Langmuir* **1996**, *12*, 145.
(19) Ainscough, A. N.; Dollimore, D. *Langmuir* **1987**, *3*, 708.
(20) Webster, C. E.; Drago, R. S.; Zerner, M. C. *J Am. Chem. Soc.* **1998**, *120*, 5509.
(21) Moyer, J. D.; Gaffney, T. R.; Armor, J. N.; Coe, C. G. *Microporous Mater.* **1994**, *2*, 229.
(22) Keir, R. I.; Lamb, D. W.; Ritchie, G. L. D.; Watson, J. N. *Chem. Phys. Lett.* **1997**, *279*, 22.
(23) CRC *Handbook of Chemistry and Physics*, 74th ed.; CRC Press: Boca Ratan, FL, 1993.

Table 6

(a) Kinetic Data ($k/(10^{-3}\ s^{-1})$) for Carbon Dioxide Adsorption on CMSA Obtained Using the LDF Model: Temperature Range 303−343 K; Pressure Range 0−100 kPa

temp/K	0−10 kPa	10−20 kPa	20−30 kPa	30−40 kPa	40−50 kPa	50−60 kPa	60−70 kPa	70−80 kPa	80−90 kPa	90−100 kPa
303	1.332 ± 0.002	2.095 ± 0.004	2.737 ± 0.010	3.264 ± 0.018	3.729 ± 0.018	4.305 ± 0.028	4.535 ± 0.033	5.102 ± 0.044	5.615 ± 0.053	5.685 ± 0.067
313	2.038 ± 0.001	2.944 ± 0.007	3.666 ± 0.016	4.373 ± 0.028	4.824 ± 0.028	5.371 ± 0.037	5.811 ± 0.050	6.427 ± 0.064	6.707 ± 0.071	7.107 ± 0.085
323	2.906 ± 0.004	3.945 ± 0.014	4.831 ± 0.026	5.580 ± 0.031	6.481 ± 0.046	7.032 ± 0.059	7.530 ± 0.073	8.389 ± 0.091	8.993 ± 0.104	8.850 ± 0.124
333	4.227 ± 0.009	5.468 ± 0.024	6.464 ± 0.029	7.369 ± 0.043	8.203 ± 0.067	8.921 ± 0.087	9.497 ± 0.098	10.016 ± 0.112	11.087 ± 0.146	11.351 ± 0.140
343	6.165 ± 0.019	7.513 ± 0.028	8.718 ± 0.045	9.569 ± 0.073	10.071 ± 0.102	11.669 ± 0.135	12.438 ± 0.138	12.453 ± 0.153	13.967 ± 0.211	14.577 ± 0.230

(b) Kinetic Data for Carbon Dioxide Adsorption on CMSA Obtained Using the Barrier Resistance/Diffusion Model: Temperature Range 303−343 K; Pressure Range 0−100 kPa[a]

temp/K		0−10 kPa	10−20 kPa	20−30 kPa	30−40 kPa	40−50 kPa	50−60 kPa	60−70 kPa	70−80 kPa	80−90 kPa	90−100 kPa
303	$k_b\ (10^{-3}\ cm\ s^{-1})$	0.0888[b]	0.195	0.320	0.425	0.600	0.710	0.900	1.100	1.050	1.050
	$k_d\ (10^{-5}\ s^{-1})$	−	1.6	1.3	1.3	1.4	1.4	1.3	1.35	1.35	1.35
313	$k_b\ (10^{-3}\ cm\ s^{-1})$	0.136[b]	0.350	0.520	0.650	0.880	1.000	1.400	1.400	1.800	2.000
	$k_d\ (10^{-5}\ s^{-1})$	−	1.6	1.6	1.7	1.5	1.6	1.5	1.5	1.4	1.4
323	$k_b\ (10^{-3}\ cm\ s^{-1})$	0.194[b]	0.47	0.70	1.07	1.60	1.80	1.90	2.20	3.30	2.70
	$k_d\ (10^{-5}\ s^{-1})$	−	2.0	1.9	1.7	1.6	1.7	1.8	1.8	1.7	1.7
333	$k_b\ (10^{-3}\ cm\ s^{-1})$	0.55	1.02	1.05	1.70	2.20	2.60	3.50	3.50	6.00	−
	$k_d\ (10^{-5}\ s^{-1})$	1.8	1.9	2.2	2.0	2.0	2.0	1.8	1.9	1.8	−
343	$k_b\ (10^{-3}\ cm\ s^{-1})$	−	1.50	2.10	2.60	3.70	4.30	6.00	6.00	8.00	−
	$k_d\ (10^{-5}\ s^{-1})$	−	2.3	2.4	2.4	2.3	2.3	2.2	2.3	2.25	2.15[c]

[a] The calculations of barrier resistance constant (k_b) and diffusion rate constant (k_d) were obtained by fitting the experimental data to the model of Loughlin et al.[13] using a particle radius of 0.2 cm. [b] Linear driving force model. [c] Fickian diffusion model.

Table 7

(a) Kinetic Data ($k/(10^{-3}\ s^{-1})$) for Nitrous Oxide Adsorption on CMSA Obtained Using the LDF Model: Temperature Range 303−343 K; Pressure Range 0−9 kPa

temp/K	0−1 kPa	1−2 kPa	2−3 kPa	3−4 kPa	4−5 kPa	5−6 kPa	6−7 kPa	7−8 kPa	8−9 kPa
303	2.399 ± 0.003	2.908 ± 0.007	3.304 ± 0.010	3.658 ± 0.015	4.003 ± 0.018	4.179 ± 0.023	4.365 ± 0.028	4.810 ± 0.035	5.000 ± 0.040
313	3.463 ± 0.006	3.960 ± 0.011	4.376 ± 0.017	4.769 ± 0.020	5.168 ± 0.027	5.486 ± 0.033	5.741 ± 0.039	6.128 ± 0.048	6.333 ± 0.052
323	4.983 ± 0.012	5.414 ± 0.018	5.889 ± 0.024	6.274 ± 0.031	6.623 ± 0.035	6.969 ± 0.043	7.241 ± 0.052	7.837 ± 0.061	8.306 ± 0.068
333	6.949 ± 0.019	7.199 ± 0.026	7.530 ± 0.034	7.949 ± 0.038	8.382 ± 0.049	8.688 ± 0.060	8.865 ± 0.070	9.033 ± 0.065	9.588 ± 0.073
343	8.726 ± 0.023	8.834 ± 0.039	9.091 ± 0.049	9.242 ± 0.051	9.671 ± 0.065	9.862 ± 0.068	10.091 ± 0.091	11.013 ± 0.108	11.124 ± 0.098

(b) Kinetic Data for Nitrous Oxide Adsorption on CMSA Obtained Using the Barrier Resistance/Diffusion Model: Temperature Range 303−343 K; Pressure Range 0−9 kPa[a]

temp/K		0−1 kPa	1−2 kPa	2−3 kPa	3−4 kPa	4−5 kPa	5−6 kPa	6−7 kPa	7−8 kPa	8−9 kPa
303	$k_b\ (10^{-4}\ _{cm\ s}-1_)$	2.25	2.8	3.85	4.7	4.9	6.3	5.5	7.2	8.3
	$k_d\ (10^{-5}\ _{s}-1_)$	2.0	2.0	1.7	1.7	1.8	1.4	1.7	1.6	1.5
313	$k_b\ (10^{-4}\ cm\ s^{-1})$	3.6	4.4	5.4	6.05	6.8	7.7	7.9	12.0	14.0
	$k_d\ (10^{-5}\ s^{-1})$	2.1	2.2	2.0	2.1	2.1	2.1	2.0	1.7	1.7
323	$k_b\ (10^{-4}\ cm\ s^{-1})$	6.0	7.0	10.0	12.0	13.0	14.0	18.0	22.0	22.0
	$k_d\ (10^{-5}\ s^{-1})$	2.4	2.4	2.1	2.0	2.0	2.0	1.9	1.8	2.0

[a] The calculations of barrier resistance constant (k_b) and diffusion rate constant (k_d) were obtained by fitting the experimental data to the model of Loughlin et al.[13] using a particle radius of 0.2 cm.

Table 8. Kinetic Data for Carbon Disulfide Adsorption on CMSA: Temperature Range 313−355 K; Pressure Range 0−0.1 kPa[a]

temp/K	$k/(10^{-6}\ s^{-1})$
313	1.1723 ± 0.0001
340	4.5482 ± 0.0004
343	4.1880 ± 0.0002
349	5.5793 ± 0.0009

[a] $E_a = 39.7 \pm 3.5$ kJ mol^{-1}. (This value does not refer to constant surface coverage and is therefore lower than the true value.[5])

was carried out using the Dubinin−Radushkevich equation

$$\log n = \log n_0 - D \log^2(p^0/p) \qquad (6)$$

where n is the amount adsorbed, n_0 is the amount adsorbed corresponding to the micropore volume, p is the pressure, p^0 is the saturated vapor pressure, and D is a constant related to the microporous structure of the adsorbent. The Dubinin−Radushkeivch (DR) plots are shown in Figure 7. It is apparent that adsorption data for carbon dioxide and nitrous oxide at 303 K give values of 3.85 ± 0.04 and 3.80 ± 0.03 mmol g^{-1}, respectively, which are similar to the value (3.71 ± 0.06 mmol g^{-1}) obtained for adsorption of carbon dioxide at 273 K. In contrast, in the case of adsorption of acetylene at 303 K, the amount adsorbed corresponding to the micropore volume was 3.44 ± 0.04 mmol g^{-1}, which is slightly lower. This lower value can be attributed to the larger size of the acetylene molecule, and since acetylene has the largest quadrupole moment of the suite of molecules studied, it is expected that its packing is less efficient than the other molecules studied. The adsorption uptakes can be compared using micropore volumes, but it is unclear as to the density of the adsorbed gases. At 303 K all three gases are close to their critical temperatures, and the densities of carbon dioxide and nitrous oxide at 303 K are 0.593 and 0.678 g cm^{-3}, respectively, while the density of acetylene at 294 K is 0.382 g cm^{-3}.[25] However in the case of carbon dioxide adsorption, it has been proposed that the density of the adsorbate at 298 K is 0.97 g cm^{-3} and similar to the density at 273 K (1.023 g cm^{-3}).[24,26] Hence there is uncertainty as to the true density of the adsorbed phase, and it is likely that the adsorbate is denser than the liquid phase at the same temperature due to the overlap of the potential energy surfaces in the microporosity. This is shown by the similarities in the amounts adsorbed corresponding to the micropore volumes for CO_2 adsorption at 273 and 303 K where the liquid densities differ by ∼50%. It is noteworthy that the graphs show a very slight degree of curvature of the DR graph as $\ln^2(p^0/p)$ approaches zero and the extrapolation represents a slight overestimate of the micropore volume. The deviations from the DR equation have been discussed in detail, and this behavior has been attributed to either part of the pore size distribution at larger pore sizes being missing or the entire microporosity is filled at a relative pressure less than unity.[27] Therefore it is difficult to establish if small differences are meaningful. Since all the isotherms were type 1, Langmuir isotherms were plotted but these graphs showed distinct curvature and therefore the description was not valid.

The surface areas obtained from the DR micropore volume data for carbon dioxide adsorption at 273 and 303 K were 418 and 434 m^2 g^{-1}, respectively, based on an area of 1.87 × 10^{-19} m^2 per molecule.[24,28] Recent electronic structure calculations using zero intermediate neglect of differential overlap (ZINDO) calculations indicate that an area of 1.916 × 10^{-19} m^2 per molecule is an alternative value for the area of a CO_2 molecule.[20] The surface areas from nitrous oxide and acetylene adsorption were not calculated because of the lack of availability of sufficiently accurate areas for molecules of nitrous oxide and acetylene. It is apparent from the isotherms that there is little or no evidence that any of the above molecules are excluded to a major extent from part of the porous structure. Therefore the adsorption kinetics are not influenced to a significant extent by differences in the accessibility of the adsorptives to the porous structure.

In all cases other than adsorption of carbon disulfide, the adsorption isotherms were compared using the virial equation approach. Comparison with virial parameters obtained for cases where the carbon was nonselective in kinetics terms showed that the values were quite similar to those obtained for adsorption on the selective CMS.[5,8,10,29] The values of A_1 for carbon monoxide, carbon dioxide, nitrous oxide, and acetylene were not strongly dependent on temperature over the temperature range studied and are similar to those reported previously for adsorption of oxygen, nitrogen, and argon on the CMS.[5,8] Cole et al. investigated the adsorption of nitrogen, argon, krypton, and xenon on various nonselective microporous carbons over the temperature range 273−398 K.[10] The values of A_1 were −(89 − 608) g mol^{-1} for nitrogen and −(46 − 2176) for argon. The values of A_1 for krypton and xenon covered a similar range. Floess et al. obtained values of A_1 in the range −(670 − 1170) g mol^{-1} for adsorption of nitrogen on microporous carbons in the temperature range 142−184 K.[29] It is apparent that there is good agreement for the virial parameters obtained in this study of selective carbon molecular sieves and those reported in previous studies on nonselective microporous carbons.

Isosteric Enthalpies of Adsorption. All the linear diatomic molecules and argon and krypton had quite similar values (18−23 kJ mol^{-1}). CO_2, N_2O, and C_2H_2 had limiting isosteric enthalpies of adsorption of 28.4 ± 0.7, 31.8 ± 0.1, and 35.0 ± 0.2 kJ mol^{-1}, respectively, at zero surface coverage. The results also show that there is no significant variation in the isosteric enthalpies of adsorption with surface coverage for all the linear molecules studied over the range of experimental conditions used except at very low surface coverage. Table 2 shows a comparison of the results with literature values for adsorption of various gases on to the graphite basal plane and microporous carbons and molecular sieves. The values reported in this paper are similar to those obtained previously for microporous carbon and carbon molecular sieves.[4,7,10,29,30] In comparison, the isosteric heats of adsorption for oxygen, nitrogen, argon, carbon monoxide, and carbon dioxide on the graphite basal plane were approximately half the corresponding values for adsorption on microporous materials. The difference was at-

(24) Rodriguez-Reinoso, F.; Linares-Solano, A. In *Chemistry and Physics of Carbon;* Thrower, P. L., Ed.; Marcel Dekker: New York, 1989, Vol. 21, p 1.
(25) *Handbook of Compressed Gases*, 3rd ed.; Van Nostrand Reinhold: New York, 1990.
(26) Garrido-Segovia, J.; Linares-Solano, A.; Martin-Martinez, J. M.; Molina-Sabino, M.; Rodriguez-Reinoso, F.; Torregrosa-Macia, R. *Langmuir* **1987**, *3*, 76.
(27) Marsh, H. *Carbon* **1987**, *25*, 49.
(28) Gregg, S. J.; Sing, K. S. W. *Adsorption, Surface Area and Porosity*, 2nd ed.; Academic Press: New York, 1982.
(29) Floess, J. K.; Kim, H. H.; Edens, S. A.; Oleksy, S. A.; Kwak, J. *Carbon* **1992**, *30*, 1025.
(30) Chihara, K.; Suzuki, M.; Kawazoe, K. *J. Colloid Interface Sci.* **1978**, *64*, 584.

Table 9. A Comparison of Structural, Physical, and Electronic Energy Parameters for the Probe Molecules[1,18−23]

molecule	critical dimension minimum cross section (pm)	Lennard-Jones (1σ) (pm)	molecule length (end-to-end) (pm)	critical temp (K)	dipole moment (μD)	$10^{40}\,\theta$ (C m^2)	molecular dimensions in 3 dimensions from ZINDO calculations (pm)		
spherical									
neon		275		44.44					
argon	384	340		150.8					
krypton		360		209.39					
linear diatomic									
oxygen	280	346		154.58		1.3	298.5	293.0	405.2
nitrogen	300	364	109.77	126.2		4.7	305.4	299.1	404.6
carbon monoxide	280		112.83	133	0.11	8.3	328.0	333.9	418.2
linear triatomic									
carbon dioxide	280	330	232	304		13.4	333.9	318.9	536.1
nitrous oxide	300		231.3	309.5	0.161	11			
carbon disulfide			310.5	552		10	353.5	337.6	665.5
linear									
acetylene			332.3	308.5		20.4			

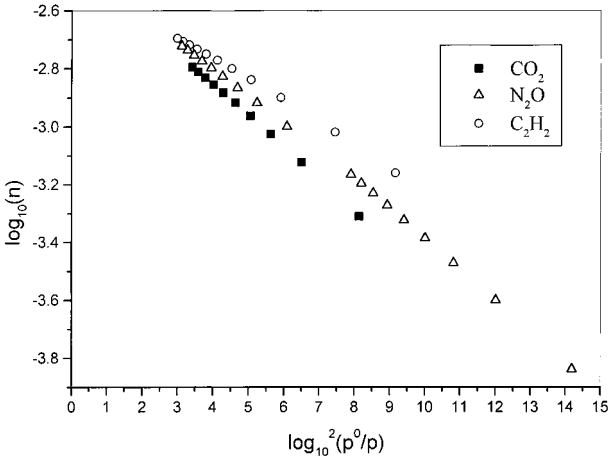

Figure 7. Dibinin−Radushkevich graphs for the adsorption of carbon dioxide, nitrous oxide, and acetylene on CMS at 303 K.

tributed to the overlap of the potential energy fields of the pore walls in the microporous materials.

Adsorption Kinetics. The adsorption kinetics for all the adsorptives except carbon dioxide and nitrous oxide on CMS A followed a linear driving force model. At low pressures and temperatures the carbon dioxide adsorption on CMS A followed an LDF model (see Figure 5a). The adsorption kinetics changed to a barrier resistance/Fickian diffusion model[13] with increasing pressure, and a Fickian diffusion model was followed for the 0.9−1 bar pressure increment at 343 K, which was the highest pressure range studied. This is the first observation of a change in kinetic adsorption mechanism with an increase in pressure.

The combined barrier resistance/diffusion model gave parameters for the barrier (k_b) and diffusion (k_d) components of the model as shown in Tables 6b and 7b for carbon dioxide and nitrous oxide, respectively. The combined barrier resistance/diffusion model was also used to describe the adsorption of neon on the CMS which also had activation energy similar to the isosteric heat of adsorption.[5] The use of the combined barrier resistance/diffusion model for adsorption of carbon dioxide over the temperature range 303−343 K and nitrous oxide at 303, 313, and 323 K shows that k_d decreases slightly with increase in pressure while k_b increases markedly with increase in pressure. The latter trend is similar to that observed for the kinetic parameters obtained from the LDF model for the other gases studied. As k_b increases with increase in pressure while k_d decreases slightly, the diffusion component becomes more important in determining the rate, and this is accompanied by an increase in the extent of curvature in the $\ln(1 - M_t/M_e)$ versus time graphs. This is expected from the graphs of $\ln(1 - M_t/M_e)$ versus time for Fickian diffusion into particles of various shapes. Molecular and Knudsen diffusion are expected to decrease with increasing pressure and molar mass of the adsorptive. Surface diffusion increases with increasing surface coverage but decreases with increasing isosteric heat of adsorption. Also, k_b increases markedly with increase in temperature whereas the increase in k_d is much less marked. In contrast, k_b and k_d showed a similar dependence on temperature for the adsorption of neon on CMS A. These observations indicate that the barrier resistance has a significantly higher activation energy than the diffusion component. Calculations for carbon dioxide and using the limited amount of data available for nitrous oxide indicate that the barrier at zero surface coverage was 50.6 ± 1.6 kJ mol^{-1} for carbon dioxide and $\sim$40 kJ mol^{-1} for N_2O. The adsorption kinetics of carbon dioxide and nitrous oxide on CMS A may have contributions from both barrier resistance and diffusion components which affect the overall kinetics. Previous studies have shown that the kinetic mechanism for a given microporous material can change from the LDF to a combined barrier resistance/diffusion mechanism with a change in the adsorptive size [Ar (340 pm) to Ne (275 pm)].[5] It is particularly interesting that it has been shown for the first time that a single adsorptive/adsorbent system shows a full range of kinetic behavior from LDF to Fickian diffusion depending on the experimental conditions used.

Comparison of Adsorption Kinetics and Surface Coverage. In all cases, the kinetic rate constants (k) increase with increasing surface coverage. The graphs of the rate constant (k) versus the amount adsorbed for oxygen, nitrogen, argon, and carbon monoxide are straight lines, but in the cases where the surface coverage is much higher (carbon dioxide, nitrous oxide, and acetylene) the corresponding graphs show a distinct curvature. A graph of $\ln(k)$ versus amount adsorbed gives a linear relation for all the adsorptives studied (see Figure 8a for data at 313 K). In the case of carbon dioxide and nitrous oxide adsorption, the parameters from the LDF model, which is only an approximate description, were used since these parameters represent an overall value for the adsorption kinetics for comparison purposes. The gradients (α) of these graphs do not vary greatly with temperature as shown in Table 10. The adsorptives which follow the LDF model have gradients (α) in the order $C_2H_2 > CO \sim Ar \sim N_2$. The variation of k_b and k_d obtained from the combined barrier resistance/diffusion model for carbon dioxide and nitrous oxide adsorption may also be considered, but these

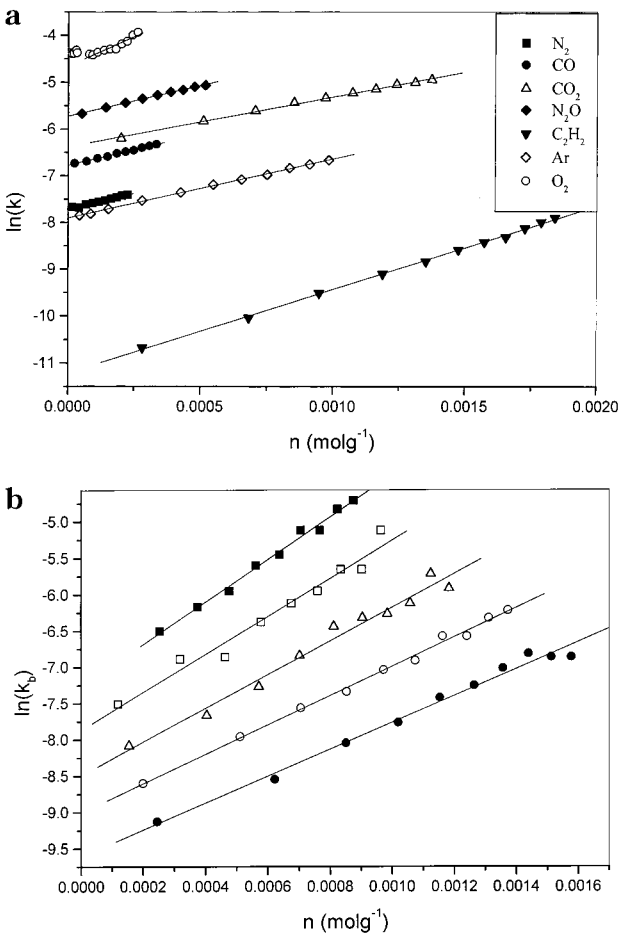

Figure 8. (a) Variation of ln(rate constant) with surface coverage (n/mmol g^{-1}) at 313 K for on CMS A: (a) carbon monoxide, (b) carbon dioxide, (c) nitrous oxide, (d) acetylene, (e) carbon disulfide, (f) argon,[5] (g) oxygen.[5] (b) The variation of ln(k_b) obtained from the combined barrier resistance/diffusion model with surface coverage(n/mmol g^{-1}) for carbon dioxide adsorption on CMS A: pressure range 0−100 kPa, temperature range 303−343 K (303 K, ●; 313 K, ○; 323 K, △; 333 K, □; 343 K, ■).

comparisons do not represent the overall kinetics. The variation of k_b with surface coverage for carbon dioxide is shown in Figure 8b. It is evident that the graphs are straight lines and are similar to the graphs for the other adsorptives which obey the LDF model. In this case it is important to separate the contributions from the barrier resistance and Fickian diffusion. This is evident from the carbon dioxide adsorption data where the value for the barrier resistance (k_b) gives a gradient approximately twice that based on using the LDF model as an approximation for comparison of the overall kinetics. Carman et al. also showed a linear dependence between ln(diffusivity) and surface coverage in the submonolayer region for the adsorption of CF_2Cl_2 on Carbolac.[31] At higher surface coverages, the diffusivity reached a maximum before decreasing slightly. The reason for this increase in rate with surface coverage is probably related to surface diffusion. Initially adsorption occurs on the most energetic sites in the microporous structure leading to the physisorption being stronger. As the surface coverage increases, the less energetic sites are occupied, the physisorption is weaker, and the surface diffusion is quicker.

There have been a number of models proposed for surface diffusion on homogeneous surfaces. Higashi developed a random hopping model[32] which was later modified to take into account multilayer effects[33−35] and developed by comparison with experimental data.[34,36,37] The difficulty in modeling the role of surface diffusion is that the CMS material is heterogeneous. The CMS was prepared by carbon deposition on a nonselective microporous substrate to introduce the kinetic selectivity. Therefore, only part of the material has molecular sieving characteristics. If the CMS pellets are subjected to a particle size reduction process, they lose their kinetic selectivity by the introduction of nonselective pathways.[3] It is not possible to estimate the pore size distribution

Table 10. Parameters from the Graphs of ln(rate constant) versus Amount Adsorbed (n/mmol g^{-1}) (a) Limiting Rate Constants at Zero Surface Coverage(k_0) and (b) Gradients(α); Temperature 303−343 K

temperature (K)	ln(k_0) (ln(s^{-1}))	α (ln(s^{-1}) mol^{-1} g)
Nitrous Oxide (from LDF model) (for comparison of overall adsorption kinetics)		
303	−6.089 ± 0.019	1217 ± 42
313	−5.717 ± 0.009	1299 ± 27
323	−5.354 ± 0.010	1338 ± 36
333	−5.006 ± 0.009	1091 ± 43
343	−4.789 ± 0.017	1043 ± 100
Carbon Dioxide (from LDF model) (for comparison of overall adsorption kinetics)		
303	−6.86 ± 0.02	1098 ± 20
313	−6.38 ± 0.02	1062 ± 21
323	−5.99 ± 0.03	1123 ± 31
333	−5.56 ± 0.02	1090 ± 28
343	−5.17 ± 0.02	1080 ± 34
Carbon Dioxide (k_b from combined barrier resistance/diffusion model)		
303	−9.61 ± 0.09	1847 ± 73
313	−9.01 ± 0.05	2021 ± 48
323	−8.49 ± 0.11	2319 ± 126
333	−7.87 ± 0.12	2614 ± 182
343	−7.27 ± 0.07	2918 ± 108
Nitrogen		
303	−8.22 ± 0.01	1349 ± 67
313	−7.71 ± 0.01	1353 ± 73
323	−7.18 ± 0.01	1203 ± 57
333	−6.70 ± 0.01	1194 ± 72
343	−6.23 ± 0.01	1151 ± 117
Argon (data from ref 5)		
303	n.d.	n.d.
313	−7.90 ± 0.01	1260 ± 14
323	−7.32 ± 0.02	1210 ± 28
333	−6.76 ± 0.03	1239 ± 58
343	−6.40 ± 0.03	1320 ± 75
Carbon Monoxide		
303	−7.30 ± 0.01	1529 ± 34
313	−6.772 ± 0.006	1341 ± 27
323	−6.304 ± 0.010	1360 ± 58
333	−5.83 ± 0.013	1235 ± 95
343	−5.38 ± 0.01	1067 ± 87
Acetylene		
303	−11.86 ± 0.05	1844 ± 35
313	−11.21 ± 0.03	1781 ± 20
323	−10.64 ± 0.05	1782 ± 17
333	−10.05 ± 0.02	1786 ± 17
343	−9.52 ± 0.02	1776 ± 17

(31) Carman, P. S.; Raal, F. A. *Proc. R. Soc. London* **1951**, *209A*, 38.
(32) Higashi, K.; Ito, H.; Oishi, J. *J. At. Energy Soc. Jpn.* **1963**, *5*, 846.
(33) Yang, R. T. Fenn, J. B. Haller, G. L. *AIChE J.* **1973**, *19*, 1052.
(34) Yang, R. T. *Gas Separation by Adsorption Processes*; Butterworths: Boston, 1987.
(35) Kapoor, A.; Yang, R. T.; Wong, C. *Catal. Rev. Sci. Eng.* **1989**, *31*, 129.
(36) Sladek, K. J.; Gilliland, E. R.; Baddour, R. F. *Ind. Eng. Chem. Fundam.* **1974**, *3*, 308.
(37) Tamon, H.; Okazaki, M.; Toei, R. *AIChE J.* **1981**, *27*, 271.

Table 11. Activation Energies and Pre-exponential Factors for Adsorption on the Carbon Molecular Sieve at Specific Surface Coverages

(a) N_2						
surface coverage/(mmol g^{-1})	0[a]	0.050	0.075	0.100	0.125	0.150
E_a/(kJ mol^{-1})	43.5 ± 0.3	43.2 ± 0.3	43.2 ± 0.3	43.1 ± 0.3	43.0 ± 0.3	42.5 ± 0.2
ln *A*	9.03 ± 0.13	9.0 ± 0.1	9.0 ± 0.1	9.0 ± 0.1	9.0 ± 0.1	8.9 ± 0.1
(b) CO						
surface coverage/(mmol g^{-1})	0[a]	0.05	0.10	0.15	0.20	0.25
E_a/(kJ mol^{-1})	41.7 ± 0.4	42.4 ± 0.6	42.3 ± 0.7	42.2 ± 0.7	42.7 ± 0.9	43.8 ± 1.2
ln *A*	9.23 ± 0.14	9.5 ± 0.2	9.6 ± 0.2	9.6 ± 0.3	9.9 ± 0.4	10.4 ± 0.5
(c) C_2H_2						
surface coverage/ (mmol g^{-1})	**0**[a]	0.60	0.75	1.00	1.20	1.30
E_a/(kJ mol^{-1})	50.7 ± 0.4	51.7 ± 1.3	51.6 ± 0.5	50.4 ± 0.4	49.9 ± 0.9	49.9 ± 1.1
ln *A*	8.25 ± 0.15	9.7 ± 0.5	9.9 ± 0.2	9.9 ± 0.2	10.1 ± 0.3	10.2 ± 0.4

Other Arrhenius Parameters at Zero Surface Coverage

	E_a	ln (*A*)	
argon	45.3 ± 2.4	9.6 ± 0.9	(data from ref 5)
carbon dioxide[b]	50.6 ± 1.6	10.4 ± 0.6	
nitrous oxide[b,c]	40.6 ± 0.5	7.5 ± 0.2	
oxygen	34.8 ± 0.5	9.0 ± 0.2	(data from ref 5)
neon[b]	34.9 ± 3.4	2.4 ± 1.3	(data from ref 5)

[a] Parameters obtained from extrapolation of graph of LDF kinetic constants versus surface coverage. [b] For k_b from the combined barrier resistance/diffusion model. [c] 303−323 K only.

accurately in this case for the following reasons: nitrogen adsorption at 77 K is not possible because of activated diffusion effects; probe molecule adsorption studies show only the porosity accessed by the probe molecule, which is limited by the selective part of the porosity.

The model for the concentration dependence of surface diffusion coefficients developed by Bhatia and Do requires a knowledge of the pore size distribution of the CMS.[38] The model predicts that at low surface coverage, the smaller pores are filled to the greatest extent. The importance of the larger pores increases with increasing surface coverage, and this leads to an increase in the effective surface diffusivity, since surface diffusivity increases markedly with pore size. Hence, the effective diffusivity increases faster than expected. This is similar to the results reported in this study.

In the case of diffusion in zeolites where pore blocking occurs, the diffusivities increase slower than expected with increase in surface coverage. This behavior has been modeled using a modification of the Higashi model to take this factor into consideration.[39]

Comparison of Adsorption Kinetics with Structural Parameters. Surface diffusion increases with increasing surface coverage due to the initial adsorption occurring on the most energetic sites and influences the adsorption kinetics.[35,36] The influence of this factor needs to be eliminated, and this is achieved by comparing rate constants as a function of surface coverage. In this case it is apparent that comparison of the kinetics of CO and CO_2 adsorption at the same pressure indicates that the adsorption of CO_2 is faster. However when the rates of adsorption of these molecules are compared on a surface coverage basis, they are similar (Figure 8a).

When adsorption characteristics are considered, in the case of slit-shaped pores, the minimum size of the molecule in one dimension is important whereas, in the case of cylindrical pores, the minimum size of the molecule in two dimensions needs to be considered. The same conclusions are reached from the data if either one or two dimensions are considered. The minimum dimensions of the two molecules obtained from electronic structure calculations using ZINDO[20] methods (see Table 9) are 328 and 333.9 pm for CO and 318.9 and 333.9 pm for CO_2. Hence it is possible to argue that this is due to a minimum size effect. Table 9 also shows the minimum dimensions obtained from ZINDO calculations for nitrogen (299.2 and 305.4 pm) and oxygen (293 and 298.5 pm). Therefore the same argument concerning the relationship between size and adsorption kinetics can be made. However comparison of the minimum molecular dimensions and adsorption of nitrogen and carbon monoxide shows that the latter is larger while the adsorption kinetics are faster (see Table 9 and Figure 8a). In addition the isosteric heats of adsorption are similar for nitrogen and carbon monoxide. It is evident that other factors are involved in determining the adsorption kinetics. Comparison of the overall kinetics for adsorption with amount of adsorption is shown in Figure 8a. Comparison of these data with the data for krypton[5] and carbon disulfide (Table 8) clearly shows that the following order is apparent: $O_2 > N_2O > CO_2 > CO > N_2 > Ar > Kr > C_2H_2 > CS_2$.

All the adsorptives follow the LDF model with the exception of carbon dioxide and nitrous oxide, which follow a combined barrier resistance/diffusion model. There is little or no evidence for exclusion of these atoms/molecules from part of the porous structure, and the isosteric heats of adsorption do not vary significantly with surface coverage. Neon has not been included in this list because the measurements refer to very low surface coverage where the isosteric heats of adsorption are higher and the very small size leads to the neon being accessible to parts of the porous structure not accessed by the other gases.[5] It is apparent from comparison of the data in Table 9 and the adsorption kinetics that the minimum dimensions of the molecules do not always provide a good guide to the adsorption kinetics. The relatively fast adsorption kinetics for N_2O and CO_2 compared with argon and N_2 indicates that the length of a molecule is not a major factor in determining the kinetics. Comparison of the adsorption kinetic results with the structural and physical parameters in Table 9 indicate that there are no simple relationships.

Comparison of Activation Energies. The activation energies at constant surface coverage are given in Table 11. To compare the activation energies for the various adsorptives, the activation energies at zero surface coverage were calculated by extrapolation of the kinetic data as a function of surface coverage. The activation energies for the data published previously[5] for the noble gases and

(38) Bhatia, S. K.; Do, D. D. *Proc. R. Soc. London* **1991**, *434*, 317.
(39) Chen, Y. D.; Yang, R. T. *AIChE J.* **1991**, *37*, 1579.

oxygen and that reported in this paper are in the order $C_2H_2 > Kr > Ar > N_2 > CO \gg O_2$ for adsorptives which follow the LDF model. In the case of carbon dioxide and nitrous oxide, which obey a combined barrier resistance/diffusion model, the activation energies for k_b are, as expected, similar to those for adsorptives which follow the LDF model while those for k_d are much lower. If the activation energies for nitrogen, oxygen, and carbon monoxide are considered in relation to the minimum dimensions of the molecules calculated using the ZINDO method, it is evident that the activation energies do not follow the expected trend, i.e., $CO > N_2 > O_2$. This is particularly interesting in the case of CO and N_2 because they have very similar electronic structures. The variation in activation energy and ln(preexponential factor) (ln(A)) with surface coverage is weak and only apparent either for those adsorptives where the surface coverage is high, outside the range of surface coverage used in this study, or at very low surface coverage where the isosteric heats of adsorption increase due to initial adsorption on the highest energy sites.[5]

Rao et al. developed a model[6,7] for the interaction potential of diffusing species in pores based on the previous model of Steele[40] for the interaction of gases with carbon surfaces. They concluded that two barriers existed, (1) entering the pore and (2) diffusing along the pore. The rate-limiting process in carbon molecular sieves was entry through the pore aperture. The study also showed that the energy barrier for pore entry for carbon dioxide was much lower than that for nitrogen. The diffusion kinetics of the gases into the porous structure is a function of the relative rates of diffusion through the barrier and along the pore. Surface diffusion is a site-to-site hopping process which depends on the height of the potential energy barrier (ΔE) which it has to overcome, and the frequency is proportional to $\exp(-\Delta E/kT)$. Everett has shown that the isosteric enthalpy of adsorption is $^1/_2RT$ higher than the maximum net attractive energy for the gas−surface interaction.[41] Hence surface diffusion is expected to decrease with increasing heat of adsorption. Surface diffusion also increases with increasing surface coverage. The LDF mass transfer parameters for oxygen, nitrogen, argon, carbon monoxide, and acetylene adsorption and the k_b kinetic parameter derived from the combined barrier resistance/diffusion model for carbon dioxide and nitrous oxide adsorption follow this trend. Molecular and Knudsen diffusions decrease with increasing pressure. This trend was observed for the values of k_d derived from the combined barrier resistance/diffusion model for carbon dioxide and nitrous oxide adsorption. Diffusion through the pore entrance depends on the height of the barrier which is characterized by the activation energy. The relative rate of the diffusion of adsorbate molecules in the porous structure and the diffusion of adsorbate molecules through the barrier are important in determining the overall adsorption mechanism. The importance of the Fickian diffusion mechanism is apparent when the change of the adsorption mechanism from a LDF to a combined barrier resistance/diffusion model is observed. This implies that diffusion along the pores which follows a Fickian diffusion mechanism becomes significant in determining the overall adsorption kinetics.

(40) Steele, W. A. *Surf. Sci.* **1973**, *36*, 317.
(41) Everett, D. H. *Trans. Faraday Soc.* **1950**, *46*, 453.

Conclusions

The results of this study clearly show that the adsorption kinetics of various probe molecules are a complex function of the size, shape, and electronic structure of the adsorptive and the interaction with selective porosity needs to be considered. It is noteworthy that the CMS used in this study is suitable for air separation but also adsorbed a wide range of adsorptives of varying sizes.

The adsorption kinetics usually followed an LDF model, but deviations occurred for carbon dioxide and nitrous oxide adsorption. It was apparent that the model for adsorption kinetics varied from LDF through combined barrier resistance/diffusion model to Fickian diffusion for carbon dioxide adsorption depending on the experimental conditions. This is the first observation of such a wide range of behavior for the adsorption dynamics of a single adsorptive/adsorbent system. The rates of adsorption increase with increasing surface coverage. A comparison of rates of adsorption for various adsorptives is only appropriate at the same surface coverage, and therefore, activation energies were calculated at constant surface coverage. Comparison of activation energies for the probe molecules shows that simplistic comparisons of size do not produce the correct order whereas comparison of critical pore dimensions where they are available do appear to give better predictions.[6,7] It is apparent that the length of the adsorptive molecules was not a factor in determining the adsorption kinetics. Comparisons of carbon monoxide and nitrogen, which are nominally isoelectronic, have similar bulk properties and, where the adsorption kinetics follow the LDF model for both adsorptives, show that carbon monoxide has faster adsorption kinetics, which are similar to carbon dioxide at the same surface coverage. This contrasts with the calculated minimum size of the molecules since both carbon monoxide and carbon dioxide are larger than both oxygen and nitrogen. It is apparent that the specific adsorbate−adsorbent interaction plays a significant role in determining the adsorption kinetics.

These results are consistent with a model which includes two factors in the adsorption dynamics in heterogeneous carbon molecular sieves: (a) diffusion along the pores; (b) diffusion through the barrier at the pore entrance. A LDF model is followed when the latter is the rate-determining step. When diffusion along the pores becomes a significant factor, the kinetic model deviates from the linear driving force model and a model based on a combined barrier resistance/diffusion is useful in describing the adsorption kinetics.

Acknowledgment. The authors thank the EPSRC for supporting this project under Grant GR/J86421 and a studentship for C.R.

LA981289P